BMC Biotechnology

RESEARCH

Open Access

Assembly of ascovirus HvAV-3h long DNA fragment using the Transformation-Associated Recombination (TAR) approach in yeast cells

Heba A. H. Zaghloul[1,3], Zhengkun Xiao[1,2], Hengrui Hu[4] and Guo-Hua Huang[1,2*]

Abstract

Background Synthetic biology is a young but rapidly growing field that allows for assembling long DNA fragments, including complete chromosomes. A key approach for long-DNA assembly is the Transformation Associated Recombination (TAR), which relies on efficient homologous recombination in yeast cells. Recent reports indicate that the TAR method efficiently assembles some human and animal viruses characterized by their large DNA genome size. The application of the TAR method to synthesize long DNA fragments derived from insect viruses is scarce. Therefore, this study aimed to explore the TAR approach for the construction of a long DNA fragment (>44.6 Kb) from the insecticidal Heliothesis virescens ascovirus 3h (HvAV-3h) dsDNA genome to assess the suitability of this approach in genome-wide engineering studies in this family of viruses.

Results The long DNA fragment assembly process involved three stages: first, we amplified 15 segments of about 2.9–3.2 Kb each via PCR. Next, we recombined these segments through three parallel TAR cycles, producing medium-sized fragments of about 15 Kb. Finally, we assembled these fragments in a single TAR cycle to form a long DNA fragment of about 44.6 kb. We identified some positive clones by colony PCR or restriction digestion pattern. To assess the quality of the assembled DNA fragment, we conducted next-generation sequencing (NGS). A comparative analysis of Sanger sequencing for medium-sized fragments and NGS data from the synthesized long-DNA fragment demonstrated a nearly matched mutation profile, suggesting that the identified mutations and deletions were present at initial synthesis. Both datasets aligned with the reference HvAV-3h strain, revealing three specific nucleotide mutations and three unique mutation regions.

Conclusions Overall, the in vivo TAR assembly method efficiently assembled a long DNA fragment derived from the ascovirus genome as a template. The process is cost-effective and can be scaled up to synthesize the entire genome for gene functional studies.

Keywords Synthetic biology, Ascoviruses, Transformation-Associated Recombination (TAR), Yeast, HvAV-3h, BAC/YAC shuttle vector

*Correspondence:
Guo-Hua Huang
ghhuang@hunau.edu.cn
[1]Hunan Provincial Key Laboratory for Biology and Control of Plant Diseases and Insect Pests, College of Plant Protection, Hunan Agricultural University, Changsha, Hunan 410128, PR China
[2]Yuelushan Laboratory, Hunan Agricultural University, Changsha, Hunan 410128, PR China
[3]Department of Botany and Microbiology, Faculty of Science, Alexandria University, Alexandria 21511, Egypt
[4]State Key Laboratory of Virology, Center for Biosafety Mega-Science, Wuhan Institute of Virology, Chinese Academy of Sciences, Wuhan 430071, China

Introduction

Synthetic biology represents a relatively young yet rapidly advancing research field integrating multiple scientific disciplines, including molecular biology, computer science, chemistry, physics, mathematics, and engineering [1]. The applications of synthetic biology are vast, particularly within virology. For example, it enables the synthesis of both RNA and DNA viral genomes. Additionally, it allows for big-scale modification of naturally existing virus genetic materials, facilitating studies on viral gene functionality, gene expression, evolution, pathogenicity, and genome architecture. Furthermore, synthetic biology can support the *de novo* synthesis of viruses without a natural genome template and the development of attenuated viruses and vaccines [1, 2]. Another interesting application of synthetic biology is the design of virus vectors with reduced immunogenicity and toxicity for gene therapy [3].

The assembly of DNA lies at the heart of synthetic biology, as it represents the most essential step for creating a fully synthetic life. In vitro, the assembly of small DNA fragments is well-established relative to long DNA fragments. For example, the in vitro assembly of long DNA fragments is limited by their high molecular weight and susceptibility to breakdown [4]. The process is known to be tedious and costly. Moreover, the chemical synthesis of long DNA fragments is error-prone [1]. Therefore, long DNA fragments are difficult to handle in vitro, and they are usually assembled in vivo by homologous recombination in host cells. The commonly used workhorses for in vivo DNA assembly are *E. coli, Bacillus subtilis*, and *Saccharomyces cerevisiae* [5, 6, 7].

The Transformation-Associated Recombination (TAR) method is increasingly adopted to assemble long DNA fragments, including entire genomes derived from viruses [8]. The TAR technology relies on the characteristic ability of yeast cells to take up and recombine the exogenous DNA efficiently. The co-transformation of two linearized DNA fragments with approximately 60 base pairs (bp) of overlapping DNA leads to recombination and ligation by homologous recombination in yeast cells [9]. Similarly, multiple DNA fragments are assembled into a Bacterial Artificial Chromosome (BAC) or Yeast Artificial Chromosome (YAC) linearized vector designed to possess 3' and 5' homologous sequences or "hook sequences" to capture the DNA fragment of interest following the same principle [10]. For example, the TAR technology efficiently assembled long DNA fragments that are 31 Kb and 55 Kb in size based on the cyanophage PP genome [11] and the monkeypox virus genome [2], respectively. Furthermore, the TAR approach facilitated the assembly of the entire genome of some animal and human viruses, including the African swine fever virus [12] and the herpes simplex virus [13], respectively.

The application of the TAR technology to synthesize long DNA fragments derived from insect viruses remains limited. For example, the only synthesized insect viral genome based on the TAR technology is the Autographa californica multiple nucleopolyhedrovirus (AcMNPV) [14]. The reason for this delay in synthesizing arthropod viruses may be due to, in part, that many insecticidal viral families such as *Ascoviridae, Poxviridae*, and *Iridoviridae* are members of the Nucleocytoplasmic Large DNA Viruses (NCLDVs). NCLDV members are considered giant viruses with large genomes (typically > 100 kb in size) and have high protein-coding capacity [45]. Therefore, genome synthesis for any viral member of the NCLDVs will be a time-consuming process and cumbersome.

Ascoviruses are among the insect viruses characterized by their large genome size. They possess relatively large circular dsDNA genomes that range in size from 100 to 200 Kb and encode 117–180 genes [15]. The virions are complex in symmetry with bacilliform, ovoidal, or allantoid (bean-like) shape and average 200–400 nm in length and 130 nm in diameter [16]. In nature, the female endoparasitic wasps are responsible for host-to-host transmission [17]. Interestingly, the infection by these insect viruses can transform the infected cell into ~ 20–30 virion-containing vesicles [18]. The accumulation of these vesicles in the infected host's hemolymph (blood) causes the disease gross pathology, which is the discoloration of the infected host hemolymph into opaque milk color [19]. The vesicles are contributing to the virus replication and transmission [19, 20, 21]. Currently, the ICTV committee (https://ictv.global/) has identified three species in the genus *Ascovirus*, namely *Spodoptera frugiperda ascovirus, Trichoplusia ni ascovirus*, and *Heliothis virescens ascovirus*.

The synthesis of long DNA fragments derived from ascovirus genomes has not yet been investigated. Therefore, in the current study, we adopted the Polymerase Chain Reaction (PCR) combined with the TAR approach to synthesize and assemble a long DNA fragment (>44.6 Kb) using the genomic DNA of Heliothis virescens ascovirus 3h (HvAV-3h), a member of the *Heliothis virescens ascovirus* species. Furthermore, we sequenced the synthesized DNA fragment by NGS to evaluate its similarity to the parental virus, thereby validating the efficacy of this approach for future large-scale studies aimed at constructing the complete viral genome of HvAV-3h or other ascoviruses. The synthesis of the entire viral genome will facilitate the gene-functional studies within this family of insect viruses.

Materials and methods

Virus, cells, and plasmid

The HvAV-3h isolated originally by [22], served as the source of the template DNA used in the series of PCR reactions conducted for the synthesis of all the small-size fragments (i.e., the building blocks of the long DNA fragment). The yeast strain (VL6-48N) used in this study is known as highly transformable with an HIS3 deletion for selection [23]. This yeast strain was the factory for the TAR of the synthesized medium-sized fragments or large-sized fragment. The yeast cells were grown on the surface of the Yeast Peptone Dextrose (YPD) medium (Qingdao Hope Bio-Technology Co.). The positive yeast colonies were selected on the surface of histidine-deficient (–His) plates. We used the *E. coli* strain EPI300 (Epicentre) [24] for the TAR cloned-vector DNA amplification. The *E. coli* cells were grown on the surface of LB agar medium supplemented with chloramphenicol (25 µg/mL) or on LB liquid medium supplemented with chloramphenicol (25 µg/mL) and copy control solution (Biosearch technologies). The TAR plasmid vector used in this study is the BAC/YAC pGF vector [11].

Virus infection and virion purification

The third instar larvae of *Spodoptera exigua* was used as a lepidopteran host for the propagation of the HvAV-3h virus particles. The larvae were grown on artificial feed and kept at 27 ± 1 °C. The larvae were exposed to 16 h of light and 8 h of dark [25]. For viral infection, we injected the third instar larvae of *Spodoptera exigua* with HvAV-3h-infected hemolymph collected and preserved at – 20 °C. After 7 days of infection, the infected larvae were bled to collect the typical milky-white hemolymph characteristic of the ascovirus infection. The collected hemolymph was exposed to sonication (100 W, 10 min, 3 s crushing, 3 s intermittent) to release the HvAV-3h virions from the virion-containing vesicles. Afterward, two milliliters of the sonicated hemolymph were added to the surface of a sucrose gradient. The sucrose gradient description and HvAV-3h virions purification method are described in [26].

Genomic DNA isolation from the purified HvAV-3h virions

After the sucrose gradient purification step of the HvAV-3h virions, the genomic DNA was isolated using the DNeasy Blood and Tissue Kit (Qiagen], according to the instructions provided by the manufacturer. The quantity and quality of the purified DNA were checked using a Nanodrop 2000 spectrophotometer (Gene Company Limited).

Polymerase Chain Reaction (PCR) amplification of 15 small-size DNA fragments from the HvAV-3h genome

The HvAV-3h purified DNA was used as a template to amplify the building blocks of the target long DNA fragment. Briefly, 30 primers were designed to amplify the target region DNA, resulting in 15 small pieces. The pieces ranged from 2963 to 3263 bp in size. The designed primers are described in Table 1. The PCR program used for the amplification of all the small-size pieces is as follows: Initial denaturation step at 98 °C for 1 min, followed by 98 °C for 10 s, 60–68 °C for 15 s, and 72 °C for 2 min, the PCR steps were repeated 30–35 times. Finally, a final extension step was conducted for 5 min at 72 °C. The reaction mixture was made following the instructions provided by the Q5 Hot Start High-Fidelity 2X Master Mix (NEB). All the PCR-amplified products were gel purified using the Monarch DNA gel extraction kit (NEB) as described by the manufacturer.

PCR modification of the 3′ and 5′ ends and mutation of the PGF vector to assemble the target fragments

The pGF vector was amplified by PCR using the primers described in Table 2. The primers were designed to possess three sections. First, 20–23 bp overlap with the ends of the BamHI-linearized pGF vector. Second, a SrfI restriction enzyme site. Third, a 40 bp overlap with the viral DNA target region. To add the SrfI site as a unique restriction position into our primers design, we first mutated the SrfI restriction site in the pGF TAR vector. We used the Q5 Site-Directed Mutagenesis Kit (NEB) for SrfI site mutation, following the instructions of the manufacturer. The destruction of the SrfI site by a substitution mutation was confirmed by Sanger sequencing of the mutated SrfI site. Finally, the amplified pGF vector (with unique 3′ and 5′ hooks) was purified from the surface of 0.8% agarose gel running in TEA buffer (1x). The quantity and quality of the purified DNA were checked using a Nanodrop 2000 spectrophotometer (Gene Company Limited). The BamHI digested pGF vector served as a template in the PCR reaction and was amplified as one piece or two overlapping pieces for subsequent assembly via TAR in yeast cells [14]. The PCR program used for the amplification of the pGF vector is as follows: Initial denaturation step at 98 °C for 1 min, followed by 98 °C for 10 s, 57 °C for 15 s, and 72 °C for 5–11 min, the PCR steps were repeated 30 times. Finally, a final extension step was conducted for 5–11 min at 72 °C. The reaction mixture was made following the instructions provided by the Q5 Hot Start High-Fidelity 2X Master Mix (NEB). All the PCR-amplified products were gel purified using the Monarch DNA gel extraction kit (NEB) as described by the manufacturer.

Table 1 Primers designed for the amplification of the small-size fragments of the Heliothis virescens ascovirus 3h (HvAV-3h), aimed at generating overlapping sequences. The sizes of the overlapping sequences in base pairs (bp) and the sizes of the PCR-amplified fragments (bp) are presented. Additionally, the primers used for colony PCR screening of the clones are listed

Primer name	Sequence 5′> 3′	Size (bp)	Overlapping (bp)
A8-1 F	GTAAAGACTCCACGAACAGTTTAATGAAAGTTTCTTC	3106	181
A8-1 R	GTCGCTTCGTCGAATTTTCGTGTTGACTAACCG		
A8-2 F	GGCGAGACATGTAGCACGACCAAATCTAAATATTC	3141	252
A8-2 R	GCCGCAAACAACTATCGACGCTACTTGATTC		
A8-3 F	CAAACCTACGTGTTCTAGATGGCACTGTATGA	3171	219
A8-3 R	GAAGAAGTGTACGATGCGGTGAGTTTGATTC		
A8-4 F	CTGATACGTTCATGTACACGCGGATATATGGAG	3179	132
A8-4 R	CATTTGTGATAGTTTATAACAGCGACGACCAG		
A8-5 F	GTGAGTTGTACTTGCCGATTTGTCGCAATAC	3263	155
A8-5 R*	GTGCTACCGTGTGAAGAACTAAAACCTATGGG		
A9-1 F*	GATCGGAATTCTCGCAACACTCTCTCATAGC	2963	233
A9-1 R	GTTAACGGGTCTGACGCATTCGAATTTTCATG		
A9-2 F	CCATCTGAAGACGATGATGATGGTAATTGTGC	3255	183
A9-2 R	CTTTGAATCGTCGAATTCGATTCGTTCTCCG		
A9-3 F	CATGAATACTACGCAACTCGGCTACGAAACG	3091	141
A9-3 R	CGAGATGTGGTCGTTTATACACTTCGTAATC		
A9-4 F	CTGTTTTCCTCGACCTAGATAACACGCTCATATG	3185	176
A9-4 R	CTAATATCCACGGCTCTACCAACGACACCGT		
A9-5 F	GAGTAAATCATGGTTAGTAATGCCAGAGTATCAG	3187	178
A9-5 R	CACGAACAACACAATCCAGAGGTGTTATACG		
A10-1 F	CTCTTATTCTCCCGTTCTGCTTTATACACGATTTTA	3105	193
A10-1 R	CATAGAGCTGCATAAGCGGTGATAAGTAAAC		
A10-2 F	ATACAGTAACGGTCTTGAAAAGAGTCGTGAAC	3153	195
A10-2 R	AACATGCTCGCAATATCGAAGTCGGTATCGTC		
A10-3 F	CGATGAATCTGACTCGGATGAATACGATGAC	3131	114
A10-3 R	GAGACTGTGGTTTTAAAGAGCGTAGAGTCACT		
A10-4 F	GTCGCGATTCAACGTATCGTTCGTTTCCGAG	3191	162
A10-4 R	GGCTTACAAGCTTATACCGCATGAGTGGAAG		
A10-5 F	GAACGAGCCATTAAAGCATAAACTCCTGGTTC	3085	–
A10-5 R	CGAAATGATACATTACAAACATCAGCTCGCT		
Vector_F*	GCAAGGCGATTAAGTTGGGTAACGCCAGG	–	
Vector_R*	GGAATTGTGAGCGGATAACAATTTCACACAGG	–	
A8-A10 R*	GACGACGACGACGACGAATGGTCTAGAAGTC	–	
A11-1 F*	GTAGATTTGTGATGGATGGCTACTATAGTGA	–	

*These primers were used for colony PCR screening of positive clones

Preparation of the highly transformable yeast strain in the spheroplast state

To transform the yeast cells with the gel-purified DNA fragments and pGF vector + hooks, we first prepared the yeast cells to be in the spheroplast stage following the protocols and buffer/solution compositions described in [24, 27]. In brief, the yeast cells were grown on the surface of the YPD agar medium for two days, followed by the inoculation of a single growing colony into a YPD liquid medium (50 mL in 250 mL Erlenmeyer flask). The cells were kept under shaking conditions for 15 h at 30 °C and 280 rpm until the O.D. 660 was about 0.2–0.25.

For spheroplast preparation, the yeast cells were collected by centrifugation at 1200 xg for 5 min in a cold centrifuge at 4 °C. Followed by suspension in 20 mL cold sorbitol solution (1 M). The sorbitol was collected by centrifugation, and the cell pellet was resuspended in 20 mL of SPE buffer supplemented with 40 µL of zymolyase and 40 µL of 2-mercaptoethanol (ME). This mixture of cells and SPE was kept under shaking conditions (60 rpm) for 15 min at 30 °C. Afterward, the cells were centrifuged using the same centrifugation conditions described above. The collected cells were gently washed twice with 50 mL of cold sorbitol solution (1 M). The cells were then collected and resuspended in 2 mL of STC solution, pH 7.5.

Table 2 Long primers designed to amplify the BAC/YAC pGF vector to add unique 3′ and 5′ hook sequences for the target DNA fragment in the HvAV-3h genome. The overlap size in base pairs (bp) between the medium-size fragments is provided

Target region	Primer name	Sequence 5′> 3′	Overlap (bp)
Part 1	pGF-F–A8	TGAGCGGTCCCATAGGTTTTAGTTCTTCACAC-GGTAGCAC**GCCCGGGC**gctagagtcgacctg-caggcatg	155
	pGF-R–A8	CCCGAAGAAACTTTCATTAAACTGTTCGTG-GAGTCTTTAC**GCCCGGGC**cgggtaccgagctc-gaattc	
Part 2	pGF-F–A9	TATGATCCGCGTATAACACCTCTGGATTGTGTT-GTTCGTG**GCCCGGGC**gctagagtcgacctgcag-gcatg	178
	pGF-R–A9	ACGTCGTTCGCTATGAGAGAGTGTTGCGAGA-ATTCCGATC**GCCCGGGC**cgggtaccgagctc-gaattc	
Part 3	pGF-F-A10	TTCGCCGGTAGCGAGCTGATGTTTGTAATG-TATCATTTCG**GCCCGGGC**gctagagtcgacctg-caggcatg	–
	pGF-R-A10	CGCATAAAATCGTGTATAAAGCAGAAC-GGGAGAATAAGAG**GCCCGGGC**cggg-taccgagctcgaattc	
pGF Vector	pGF-F*	TCGTCTCGCGCGTTTCGGTGATGACG	–
	pGF-R	GTCTGCTCCCGGCATCCGCTTACAGAC	

*The pGF-F and pGF-R primers were used for the amplification of the pGF vector with the long primers to amplify the vector as two fragments

Co-transformation of the DNA fragments and linearized pGF vector into yeast spheroplasts

Finally, the DNA gel-purified fragments (~100–200 ng) and linearized vector (~100 ng) were mixed with the freshly prepared spheroplasts (described above) [24, 27]. Afterward, we added 800 µL PEG8000 solution and mixed it gently by inverting the tube 4–6 times. This mixture was incubated at room temperature for 10 min. The cells were collected by centrifugation at a low speed of 400 xg at 4 °C. The collected cells were resuspended in 800 µL of SOS solution, followed by 40 min of static incubation at 30 °C. The yeast cells were cultured on histidine-deficient (–His) plates and kept at 30 °C for 3 days to check the growing yeast clones. The obtained yeast clones were slightly touched with a sterile tip and added separately into the pre-set PCR mixture to examine by colony PCR the presence of the assembled fragments in the examined colony. For the colony PCR, the clones were examined using the same primers used to amplify the small-size fragments or using primers that span the junction between the DNA fragment and the vector or internal junction between two fragments (Table 1) to confirm that all the synthesized pieces are present in the final construct. Afterward, All the PCR reaction products were examined on the surface of 0.8% agarose gel in 1X TEA running buffer.

Plasmid preparation from yeast and *E. coli* cells

The positive yeast clones identified by colony PCR screening were cultured on SD-His liquid medium for two days (at 200 rpm and 30 °C). The growing yeast cells were collected by centrifugation (~3 mL), followed by treatment with 25 µL of zymolyase and 2.5 µL of beta-mercaptoethanol to remove the yeast cell wall [12]. After one hour of static incubation at 37 °C, we isolated the yeast plasmid DNA following the instructions of the GeneJET plasmid Miniprep kit (Thermo Scientific). For plasmid isolation from *E. coli* cells, the cells growing on the LB liquid medium supplemented with chloramphenicol (25 µg/mL) and copy control solution were used for plasmid preparation using the same kit. The *E. coli* cells were grown for 5–12 h at 37 °C and 200–240 rpm.

Electroporation of *E. coli* cells

To amplify the yeast-purified plasmids, we transferred each plasmid into electrocompetent *E. coli* EPI300 cells prepared and preserved at–80 °C. Briefly, 3–6 µL of each purified plasmid were mixed gently with 40–60 µL of competent cells and incubated on ice for 5 min. Afterward, we added this mixture into a 0.2 cm pre-chilled electroporation cuvette. The electroporation was conducted at 2.5 kV, 25 µF, and 200 Ω. The pulsed cells were immediately transferred into 1 mL SOC medium and incubated on a shaker incubator for 1–2 h at 37 °C and 180 rpm before being cultured on the surface of fresh LB medium supplemented with chloramphenicol (25 µg/mL).

Restriction digestion analyses of the intermediate and long-assembled DNA fragments

The constructs were analyzed by restriction digestion to confirm the insert size. The purified plasmids were digested with SrfI or HindIII (NEB) restriction enzymes in case of intermediate or long DNA fragments, respectively. The mutated pGF plasmid (described above) was digested with SrfI to confirm the length of the synthesized intermediate DNA fragments. On the other hand, HindIII was used to digest the long DNA fragment (final construct) to confirm the digestion pattern and to validate its similarity to the in silico predicted pattern.

Sanger-sequencing and NGS of the synthesized fragments, followed by a comparison with the parental viral DNA sequence

The three medium-sized fragments were sequenced by a Sanger sequencer through the sequencing service provided by I-congene (Wuhan, China). The sequence of the long-DNA fragment was conducted through the Beijing Tsingke Biotech Co., Ltd. Briefly, the long-DNA fragment was processed using the MiSeq Reagent Micro Kit V2, according to the manufacturer's instructions, followed

by Illumina Miseq sequencing. The obtained reads were cleaned by fastp (0.20.1) filtering. The DNA assembly was made by spades.py using the HvAV-3h strain (KU170628) as a reference genome. The assembled sequences were aligned with the HvAV-3h genome by dot-blot analysis, or BLAST searched with other ascoviruses available in the NCBI database to identify the degree of sequence identity and mutations. The dot plot was generated through the BLASTn tool available through the NCBI. Briefly, we aligned the parental viral genome sequence located from nucleotide 96,478 to nucleotide 141,151 in the HvAV-3h genome (NCBI accession no. KU170628) with the NGS assembled sequence of the synthesized fragment. We used the default alignment parameters suggested by the BLASTn tool. The generated dot-plot y-axis refers to the HvAV-3h wild-type sequence, while the x-axis refers to the synthesized fragment sequence.

Results

Assembly of the 44,674 bp fragment derived from the HvAV-3h DNA genome

To synthesize the long DNA fragment (size = 44,674 bp) located from nucleotide 96,478 to nucleotide 141,151 in the HvAV-3h genome, we followed the approach described in Fig. 1. Briefly, the TAR approach was applied sequentially to assemble the long-DNA fragment. First, the PCR-synthesized overlapping DNA small-size fragments were recombined in yeast cells using TAR to assemble three intermediate-size fragments by homologous recombination, followed by a second round of TAR in yeast cells to synthesize the long-DNA fragment. The linearized pGF vector, with specific 3' and 5' hooks, was transformed along with the small-size or intermediate-size fragments into the yeast spheroplasts. The target HvAV-3h DNA region encodes 42 proteins, including eight bro-like proteins, 18 hypothetical proteins, three

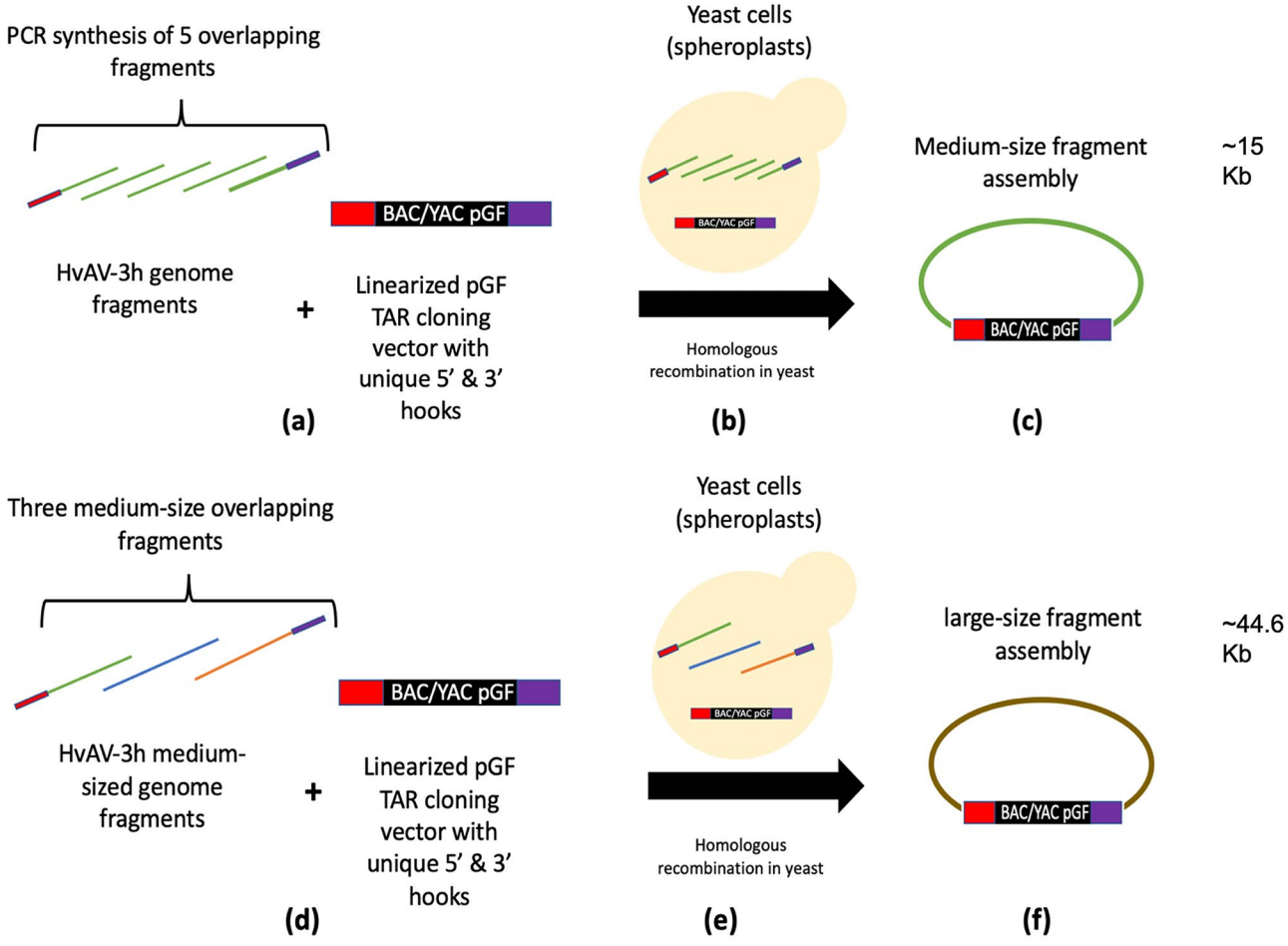

Fig. 1 The flowchart for assembling the target long DNA fragment derived from the Heliothis virescens ascovirus 3h (HvAV-3h) genome. The assembly of the long DNA fragment was conducted in a hierarchical process where the PCR synthesized overlapping DNA small-size fragments (~2.9–3.2 Kb) (**a**) were co-transformed with the BAC/YAC shuttle pGF vector into yeast spheroplasts for assembly in three parallel rounds of Transformation-Associated Recombination (TAR) in yeast cells (**b**) to form three intermediate-size (~15 Kb) fragments (**c**). Afterward, a final TAR cycle is made in yeast cells (**d** and **e**) to recombine the three intermediate fragments into a single long DNA fragment (**f**). The 3' and 5' unique hooks are referred to by purple and red color, respectively

ATPases, a cathepsin B protein, a helicase protein, a BRCA1-like protein, a gamma-glutamyl hydrolase-like protein, a serine/threonine protein kinase, a CDT phosphatase transcription factor, a nicotinate-nucleotide pyrophosphorylase, a NAD-glutamate dehydrogenase, a thioredoxin-like protein, a putative zinc-finger DNA binding protein, a transcription elongation factor S–II, a lysophospholipid acetyltransferase, and a lectin-like protein.

Synthesis of the small-size fragments and vector amplification

The first step in DNA synthesis was to amplify the small size overlapping fragments or the building blocks. The overlap ranged from 114–252 bp between the small-size fragments to facilitate recombination in yeast cells (Table 1). We conducted a series of PCR reactions to synthesize the small DNA fragments. In total, we synthesized 15 small-size (Ranging in size from 2963 to 3263 bp) fragments using PCR, and the primers used for each piece amplification are described in Table 1. The size of the PCR amplified fragments was checked on the surface of Agarose gel (Fig. 1). The gel-purified small-size fragments were prepared and co-transformed with linearized pGF vector, amplified by PCR to possess unique 3' and 5' hook sequences (Fig. 2a). Every five fragments represent one part that is intermediate in size (i.e., three parts in total to form the long DNA fragment). The small-size fragments located at nucleotide 96478 to 111553 in the HvAV-3h genome represent part 1 (15,076 bp in length), the small-size fragments located at nucleotide 111399 to 126346 represent part 2 (14,948 bp in length), and the small-size fragments located at nucleotide 126169–141151 represent part 3 (14,983 bp) (Fig. 2b–d).

Assembly of three intermediate-size fragments (Parts 1, 2, and 3)

To assemble the first intermediate-size fragment (Part 1), the yeast spheroplasts were transformed with the first set of small-size fragments that constitute part 1 (~15 Kb) (Fig. 2b) along with the linearized pGF vector two fragments (Fig. 2a). Similarly, we assembled part 2, and part 3, individually, using the related small-size fragments (Fig. 2c and d). We isolated the plasmids from putative-positive yeast colonies growing on–His selective medium and transformed them into electrocompetent *E. coli* cells for amplification. The plasmids were then isolated from the transformed *E. coli* cells. The assembled intermediate-size fragments derived from part 1, part 2, and part 3 were released from the purified pGF vectors as demonstrated in Fig. 3a using the SrfI restriction enzyme. The SrfI restriction enzyme was added to our primers design (Table 2) to facilitate the release of the intermediate-size and large-size fragments after assembly. A substitution mutation was successfully made in the pGF SrfI restriction site, as confirmed by Sanger sequencing described in Fig. 3b. The mutation destroyed the pGF original SrfI site to become a unique-cutting site for the subsequent release of the assembled fragments.

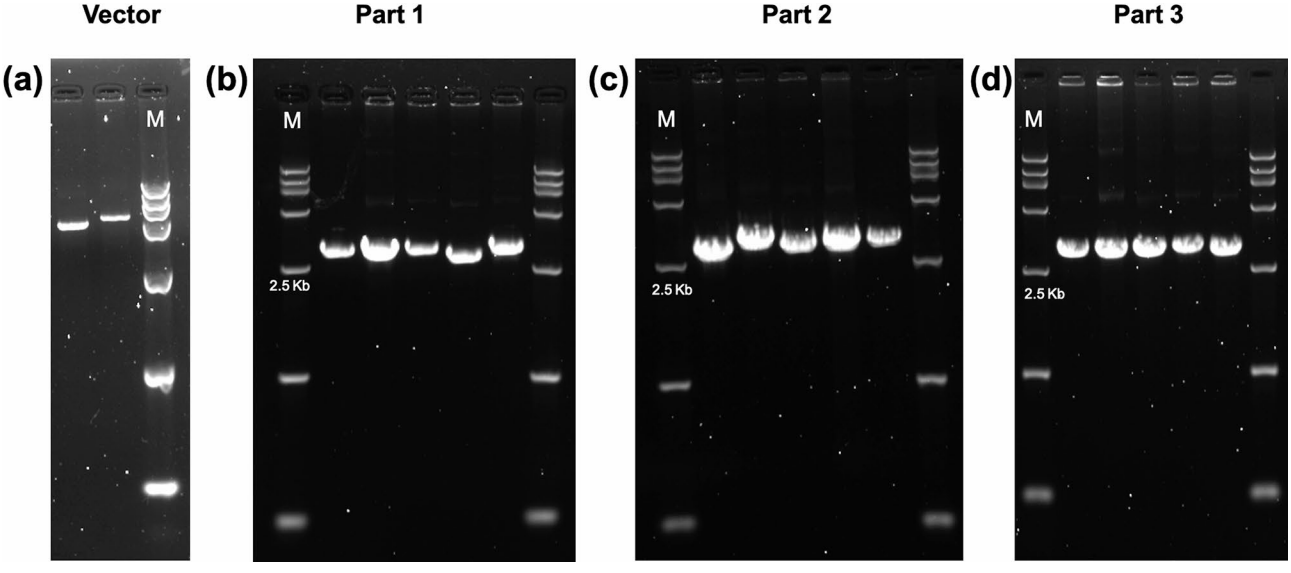

Fig. 2 PCR amplification of the BAC/YAC shuttle pGF vector and small-size DNA building blocks of the Heliothis virescens ascovirus 3h (HvAV-3h) long DNA fragment. In **a**, the pGF vector is amplified by PCR in the form of two overlapping fragments to be recombined in yeast cells via Transformation-Associated Recombination (TAR). In **b**, **c**, and **d**, the gel images refer to the PCR amplified small-size fragments using the purified viral DNA as a template in PCR reactions. **Part 1** refers to the first set of small-size fragments located at nucleotide 96478 to 111553, **part 2** refers to the second set of small-size fragments located at nucleotide 111399 to 126346, and **part 3** refers to the third set of small-size fragments located at nucleotide 126169–141151. The described nucleotide positions are based on the HvAV-3h genome sequence (NCBI accession No. KU170628)

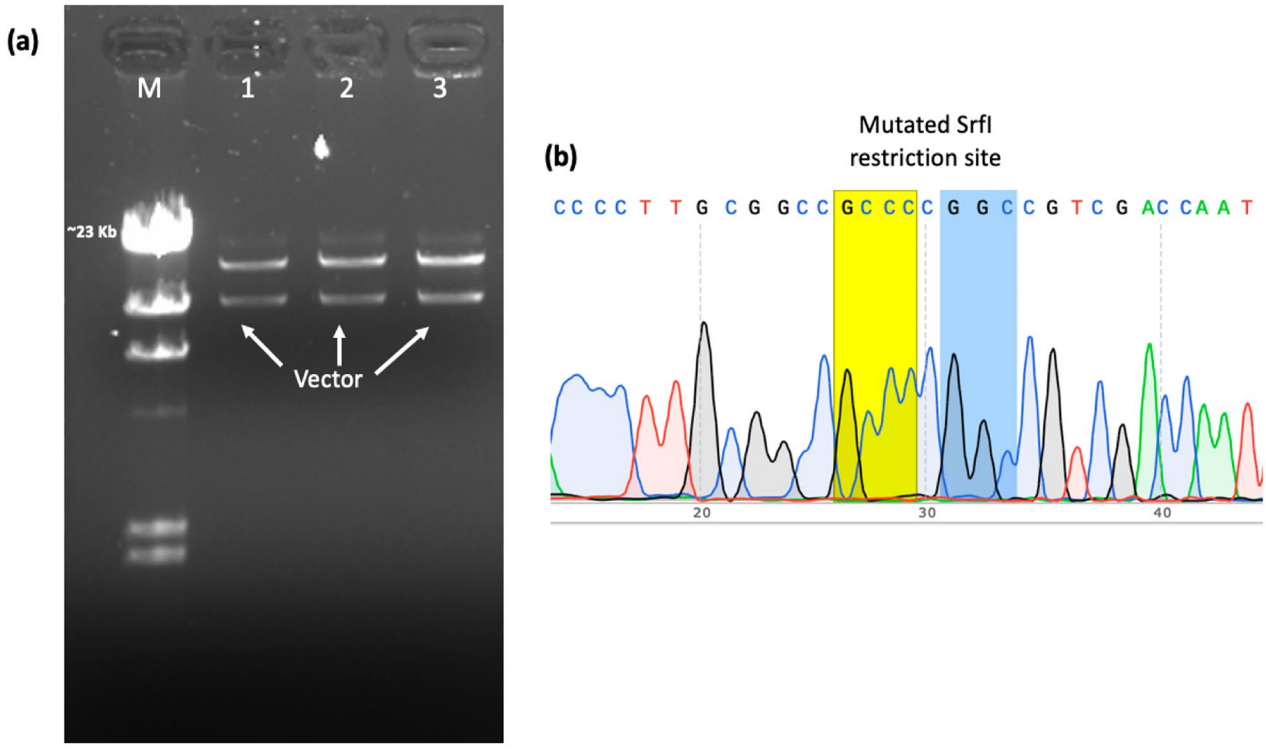

Fig. 3 Restriction digestion of the recombined pGF plasmid to release the intermediate-size assembled fragments. In (**a**), the three intermediate-size fragments assembled separately via TAR in yeast cells from the small-size PCR amplified fragments were released from the pGF vector using a unique restriction enzyme site (SrfI). In (**a**), note the presence of a faint band in lanes 1, 2, and 3 higher in size than the assembled intermediate fragment (~15 Kb) and the vector (~10 Kb) referring to the incomplete digestion with SrfI. In (**b**), the Sanger sequence validation of the SrfI restriction site (GCCCGGGC) mutation in the pGF vector. The plasmid was mutated to facilitate the release of the assembled fragments by SrfI digestion

The assembly of the long DNA fragment from the three intermediate-size fragments

After the SrfI digestion, we observed the incomplete digested vector (described in Fig. 3a). The presence of an incomplete digested vector interfered with the subsequent trials to recombine the three intermediate fragments. Therefore, we conducted a triple digestion using other unique-cutting restriction enzymes like SbfI and FseI. These two restriction sites exist only in the pGF vector and are absent in the viral DNA part1, 2, and 3 assembled fragments. The vector destruction step was essential to get any yeast-positive clones that assembled the three parts. For example, although we got several yeast colonies (>300) growing on the selective–His plates, they were only possessing one part and missing the other two, implying that they were false-positive clones formed due to the presence of some circularized pGF vector-loaded with one intermediate fragment. On the other hand, the gel purification of the three intermediate fragment parts 1, 2, and 3 (Fig. 3) and co-transformation with the linearized pGF vector improved the efficiency of the final TAR process to assemble the long-DNA fragment and getting positive clones (Fig. 4). The detection of the positive yeast clones relied on the colony PCR screening of some yeast colonies. Figure 4a demonstrates the examination of ten clones. In all clones, we were able to detect the first junction between the vector and the long DNA fragment, described in Fig. 4c. Moreover, further examination of two randomly selected clones with other primer sets designed to confirm the presence of the second junction between the vector and the long-DNA fragment or internal junction between two assembled fragments was positive as well (Fig. 4b), implying the assembly of the full-size long DNA fragment in the two clones.

The assembled long DNA fragment shares a high sequence identity with HvAV-3h and other closely related HvAV strains

Subsequently, we transformed the long DNA fragment assembled and cloned in the pGF vector into electrocompetent cells for a final round of plasmid DNA amplification. A limited number of clones (1–2 clone/plate) was able to grow on the surface of the LB + cm selective plates, implying a reduction in the *E. coli* transformation efficiency with increasing the transformed plasmid size. Analysis of these clones by restriction digestion using HindIII indicated that the resulting digestion pattern closely matched the in silico predicted pattern for

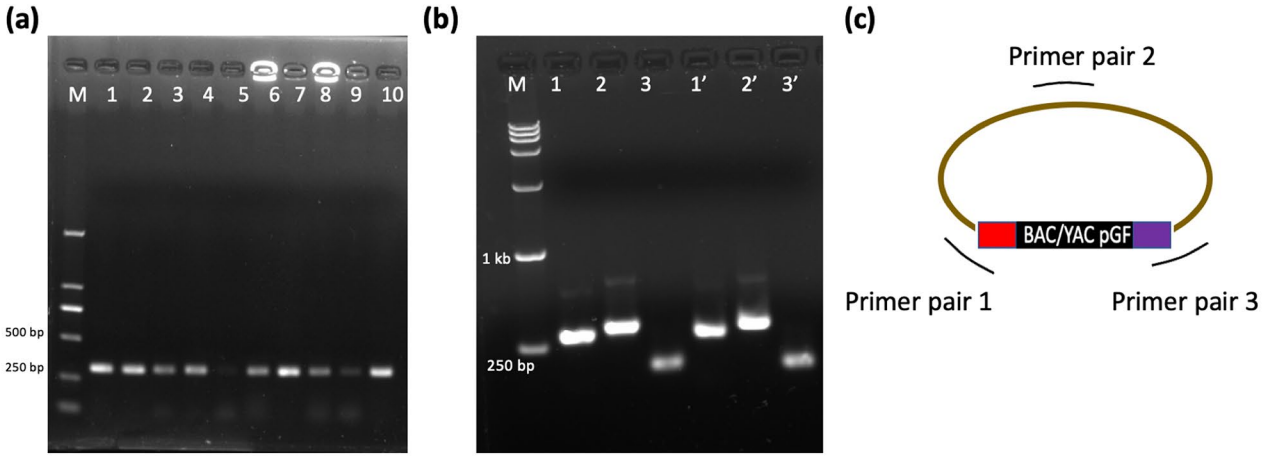

Fig. 4 PCR screening of positive yeast clones. Panel (**a**) displays the results of colony PCR conducted on putative positive colonies transformed with gel-purified HvAV-3h fragments with the linearized pGF vector, which contains unique 3′ and 5′ hooks (Lanes 1–10). Panel (**b**) shows the recombined plasmid DNA from two randomly selected yeast clones, which were subsequently analyzed using PCR with three distinct sets of primers. The positions of these primers are depicted in panel (**c**). Primer pair 1 is at the first junction between the pGF vector and the assembled HvAV-3h long DNA fragment. Primer pair 3 is at the second junction between the pGF vector and the assembled HvAV-3h long DNA fragment. Primer pair 2 is at the region connecting two intermediate pieces. The PCR products from the first and second yeast clones are presented in lanes 1–3 and lanes 1′–3′, respectively

this region in the parental HvAV-3h genome (Fig. 5a). We performed NGS for the verified plasmid. The sequence of the long-DNA fragment (A8-A10) synthesized in this paper has been deposited in the NCBI BioProject database accession no. (PRJNA1230813). The NGS and dot-plot analysis of the obtained long DNA fragment sequence with the wild-type HvAV-3h genome in the target region (located from nucleotide 96,478 to nucleotide 141,151) revealed a 97.3% sequence identity between the compared sequences. Moreover, the dot-plot analysis revealed the presence of a deleted region containing a bro-like gene. Specifically, we detected the deletion of bro11, two small-size hypothetical proteins, and a nicotinate-nucleotide pyrophosphorylase protein in the synthesized fragment (Fig. 5b). Generally, this deleted region in HvAV-3h genome (105–109 Kb) exhibits substantial variation across different HvAV strains (Fig. 5c). Furthermore, the pairwise alignment with HvAV-3h (NCBI accession No. KU170628) revealed the presence of multiple mutations in the synthesized fragment. However, most of these mutations were synonymous and are unlikely to be caused solely by TAR.

Interestingly, conducting a comparative analysis of Sanger sequencing results for the medium-sized fragments and NGS data from the synthesized long-DNA fragment demonstrated nearly identical mutation profiles. This consistency indicates that the detected mutations/deletions were already present during the initial synthesis of medium-sized fragments. Alignment of both sequencing datasets with the reference HvAV-3h strain (KU170628) revealed three specific nucleotide mutations (Table 3) and three mutation regions (Fig. 5c): The first mutation region (105–109 kb) is the segment with the substantial variation across different HvAV strains (Fig. 5c). The BLAST result showed that the synthesized fragment has the maximum query coverage with HvAV-3g and the highest sequence identity with HvAV-3e (Supplementary Table 1). In the second mutation region (113–114 kb), the BLAST analysis demonstrated 99.8% sequence consistency with HvAV-3i (Supplementary Table 2). The third mutation region (122.2–122.4 kb) showed complete sequence identity with both HvAV-3i and HvAV-3e strains (Supplementary Table 3).

Discussion

The assembly of long DNA fragments derived from any member of the *Ascoviridae* family has not been previously investigated. Therefore, the current study aimed to apply the TAR assembly method to assemble a long DNA fragment derived from the HvAV-3h, which belongs to this family of insect viruses characterized by their large dsDNA genomes and complex symmetry [15]. Evaluating assembly methods using DNA templates derived from diverse organisms may reveal the strengths and weaknesses of a specific approach in large-scale synthetic genomics for a particular virus species or family. Many insect viruses possess large dsDNA genomes and belong to the NCLDVs, which are recognized to have the most complex known viruses. Notable arthropod-infecting families within this group include *Ascoviridae, Iridoviridae*, and *Poxviridae* [28]. In addition to arthropods, the *Iridoviridae* can infect fish and Amphibia [19], whereas *Poxviridae* are capable of infecting vertebrates. NCLDVs are typically distinguished by their large genomes,

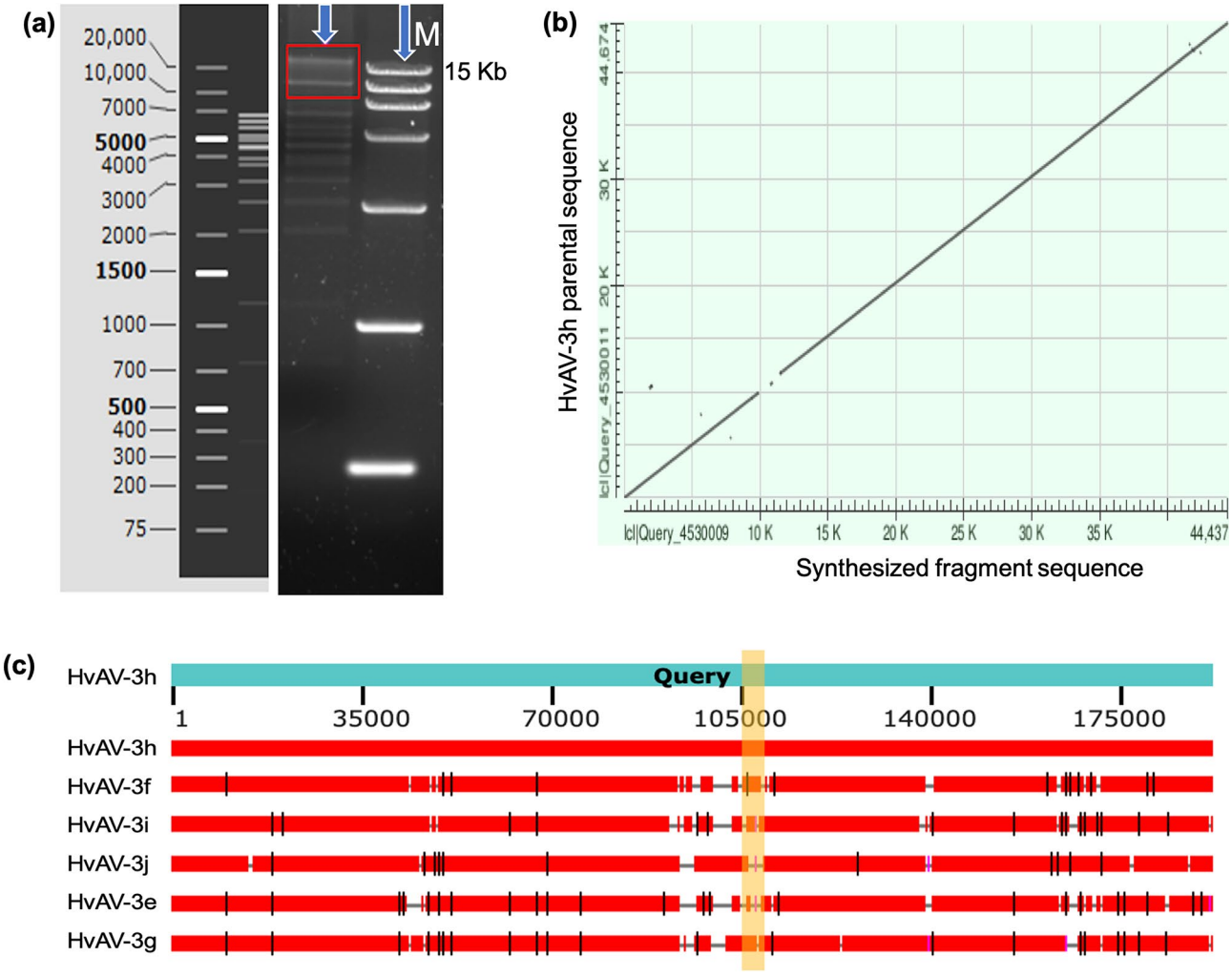

Fig. 5 Restriction digestion pattern analysis of the synthesized long-DNA fragment, dot-plot analysis of its next-generation sequence with parental HvAV-3h, and BLAST alignment with other HvAV strains. In (**a**) HindIII digestion pattern of the synthesized long DNA-fragment recombined to pGF plasmid. M refers to the molecular DNA marker (250 bp-15 Kb size range, Accurate Biology). The left-side pattern represents the in silico prediction, and the right-side pattern refers to the resulting HindIII digestion pattern. The resulting digestion pattern closely matched the in silico predicted pattern for this region in the parental HvAV-3h genome except for the portion highlighted by the red box. These bands may represent incomplete digestion or mutation in the HindIII restriction site. In (**b**), dot-plot analysis of the synthesized long DNA fragment with the parental Heliothis virescens ascovirus 3h (HvAV-3h) genome sequence in the target region (located from nucleotide 96,478 to nucleotide 141,151). The y-axis represents the HvAV-3h parental viral genome (NCBI accession No. KU170628). The x-axis represents the synthesized fragment obtained NGS sequence. In (**c**), a diagram of BLAST result of querying HvAV-3h whole genome. The 105–109 kb region exhibiting substantial variation across different HvAV strains was labeled by an orange box

Table 3 Point mutations in synthesized long-DNA fragment and medium-sized fragments

Position*	HvAV-3h	Synthesized long-DNA fragment	Medium-size fragments
111,130	C	T	C
115,448	C	T	T
124,145	G	A	A

*The position is referred to the genome of HvAV-3h (NCBI accession No. KU170628)

virions, and protein-coding capacity, such that the size and coding capacity of these viruses can be comparable to those found in bacterial genomes [45].

We successfully generated a single long DNA fragment derived from the HvAV-3h genome, constituting approximately 23.5% of the total genome size (190,519 bp). Notably, this long DNA fragment exceeds the lengths of the complete genomes of several other synthesized viruses, for example, hepatitis C virus (HCV), SARS-like coronavirus, and bacteriophage T7 [29, 30, 31]. Recent studies demonstrated that the TAR approach is among the promising DNA assembly methods that specifically facilitate the assembly of long DNA fragments. It requires no

enzymes and produces seamless ligated DNA fragments by yeast homologous recombination [2, 11, 32]. In our study, we constructed the long DNA fragment in a gradual process by synthesizing small fragments, which were recombined into intermediate-sized fragments by TAR in yeast. Afterward, we made an additional round of TAR in yeast cells to assemble the intermediate fragments. Previous experiments have demonstrated the possible usage of TAR to form a large circular DNA molecule from over 20 DNA fragments in a single transformation step in yeast cells. However, one limitation associated with the direct assembly of the final long DNA construct using small fragments is that the yeast cell must take up at least one of each small fragment to assemble the complete long DNA fragment [33]. Consequently, as the number of DNA pieces required for uptake increases, the probability of successful assembly diminishes.

Previous studies have indicated that only a limited number of mutations existed in the viral genome fragments assembled by TAR in yeast cells [13, 34, 44]. In contrast, we have observed the presence of a bro-like gene containing region deletion and the accumulation of multiple synonymous mutations in the synthesized long DNA fragment. Moreover, we observed that the long-DNA fragment NGS sequence had a nearly identical mutation profile with the assembled medium-sized fragments. This consistency indicates that the detected mutations and deletions were already present during the initial synthesis of medium-sized fragments. Therefore, the presence of these deletions and mutations in the case of HvAV-3h DNA fragment synthesis is unlikely to be caused solely by TAR and could reflect the contribution of different factors. For example, the presence of the template viral DNA as a cocktail resulting in that some of the 2–3 Kb fragments generated by PCR already carrying the mutation. Among the possible reasons for the existence of these viruses as a cocktail of closely related strains is the difficulty of separating them due to the typical propagation of ascoviruses in different lepidopteran insect hosts and the lack of a suitable insect tissue culture system to reproduce the in vivo infection and to get a singular viral clone. For example, the ascovirus characteristic virion-containing vesicles were reported by previous in vitro tissue culture studies to be absent or formed with significant differences when compared to the in vivo formed ones [35]. Interestingly, a similar observation was reported earlier in the Spodoptera frugiperda ascovirus 1a (SfAV-1a) during an in vivo transcriptomic study, where mapping of the SfAV-1a reads into the reported viral genome sequence, including the Open Reading Frames (ORFs) demonstrated the presence of multiple mismatches [36]. These observations may explain why most of the mutations we have identified in the synthesized long-DNA fragment were synonymous. On the other hand, the template viral DNA may have encountered the accumulation of multiple mutations due to the repeated passage of the parental viral DNA through different insect hosts, which facilitates the accumulation of these synonymous mutations. A recent study on HvAV-3h supports this hypothesis since the HvAV-3h virions adapt to the host. For instance, the HvAV-3h virions exhibited different protein compositions when isolated from different host larval species [37]. Generally, DNA viruses exhibit higher mutation rates relative to RNA viruses. The significance of these synonymous mutations for virus evolution remains controversial. Nonetheless, these mutations can alter cis-acting regulatory elements, reduce the stability of duplex structures, and affect gene expression [38, 39, 40, 41]. Additionally, some mutations may occur during the amplification step of the TAR assembly building blocks synthesized by PCR. Indeed, even with PCR enzymes characterized by their high fidelity, random errors are inevitable, particularly during amplifying long DNA sequences [11, 42, 43]. To mitigate mutation introduction during TAR, some researchers have used exclusively chemically synthesized DNA building blocks, thereby preventing the introduction of any mutation in the assembled long fragments [44]. Moreover, cloning and Sanger sequencing of the small-building blocks can contribute to excluding mutated fragments at early synthesis steps.

Conclusions

We successfully used the TAR assembly approach to construct a long-DNA fragment derived from the HvAV-3h genome. The findings of this study revealed the efficient and cost-effective synthesis of both small (~2.9–3.2 Kb) and intermediate-sized (~15 Kb) viral DNA fragments to assemble the final construct exceeding 44.6 Kb. However, a decrease in the transformation efficiency of *E. coli* was encountered when the transformed plasmid size increased. In summary, this method holds the potential for scaling up to synthesize the complete viral genome for gene functional studies.

Acknowledgements

We would like to extend our gratitude to Prof. Gengfu Xiao, Prof. Zhihong Hu, and Prof. Manli Wang, Wuhan Institute of Virology, Chinese Academy of Sciences, Wuhan, China for providing us with the yeast cells, bacterial cells and plasmid. Moreover, we would like to extend our acknowledgement to Dr. Han Xiao, Wuhan Institute of Virology, Chinese Academy of Sciences, Wuhan, China for his technical advice and support during the conduction of this study.

Author contributions

H.A.H.Z.: Conceptualization, Methodology, Visualization, Formal analysis, Data curation, Writing-original draft, Writing-reviewing and editing, Project administration, and Funding acquisition. Z.X: Methodology, Visualization, Formal analysis, Data curation, and Writing-reviewing and editing. H.H: Formal analysis, Writing-reviewing and editing. G.H.H: Writing-reviewing and editing, Supervision, Project administration, and Funding acquisition. All authors reviewed the manuscript.

Funding
This work was funded by the National Natural Science Foundation of China (grant number 32250410311) provided to Heba A. H. Zaghloul and China Agriculture Research System (grant number CARS-23-C08) provided to Guo-Hua Huang.

Data availability
All the data and materials are provided in the main manuscript.

Declarations

Ethics approval and consent to participate
Not Applicable

Consent for publication
Not Applicable

Competing interests
Authors declare that they have no competing interests.

Received: 14 January 2025 / Accepted: 1 April 2025
Published online: 22 May 2025

References

1. Wimmer E, Mueller S, Tumpey TM, Taubenberger JK. Synthetic viruses: a new opportunity to understand and prevent viral disease. Nat Biotechnol. 2009;27:1163–72.
2. Yang L, Tian L, Li L, Liu Q, Guo X, Zhou Y, Pei R, Chen X, Wang Y. Efficient assembly of a large fragment of monkeypox virus genome as a qPCR template using dual-selection based transformation-associated recombination. Virol Sin. 2022;37:341–47.
3. Mirkovitch J. The Role of Synthetic Virology in Developing Vaccines and Antiviral Therapies. J Curr Synth Syst Biol. 2023;11:32.
4. Tan W, Miao Q, Jia X, Liu Y, Li S, Yang D. Research Progress on the Assembly of Large DNA Fragments. Chembiochem. 2024;25.
5. Juhas M, Reuss DR, Zhu B, Commichau FM. *Bacillus subtilis* and *Escherichia coli* essential genes and minimal cell factories after one decade of genome engineering. Microbiology (Reading). 2014;160:2341–51.
6. Blount BA, Weenink T, Ellis T. Construction of synthetic regulatory networks in yeast. FEBS Lett. 2012;586:2112–21.
7. Juhas M, Ajioka JW. High molecular weight DNA assembly in vivo for synthetic biology applications. Crit Rev Biotechnol. 2017;37:277–86.
8. Kouprina N, Larionov V. Transformation-associated recombination (TAR) cloning and its applications for gene function; genome architecture and evolution; biotechnology and biomedicine. Oncotarget. 2023;14:1009–33.
9. Noskov VN, Koriabine M, Solomon G, Randolph M, Barrett JC, Leem SH, Stubbs L, Kouprina N, Larionov V. Defining the minimal length of sequence homology required for selective gene isolation by TAR cloning. Nucleic Acids Res. 2001;29:E32.
10. Kouprina N, Larionov V. Transformation-associated recombination (TAR) cloning for genomics studies and synthetic biology. Chromosoma. 2016;125:621–32.
11. Hou Z, Zhou Z, Wang Z, Xiao G. Assembly of long DNA sequences using a new synthetic Escherichia coli-yeast shuttle vector. Virol Sin. 2016;31:160–67.
12. Labroussaa F, Mehinagic K, Cippa V, Liniger M, Akarsu H, Ruggli N, Jores J. In-yeast reconstruction of the African swine fever virus genome isolated from clinical samples. STAR Protocols. 2021;2:100803.
13. Xiao H, Hu H, Guo Y, Li J, Wen L, Zeng W, Wang M, Luo M, Hu Z. Construction and Characterization of a Synthesized Herpes Simplex Virus H129-Syn-G2. vol. 38. Virol Sin; 2023. p. 373–79.
14. Shang Y, Wang M, Xiao G, Wang X, Hou D, Pan K, Liu S, Li J, Wang J, Arif BM, et al. Construction and Rescue of a Functional Synthetic Baculovirus. ACS Synth Biol. 2017;6:1393–402.
15. Asgari S, Bideshi DK, Bigot Y, Federici BA, Cheng X, ICTV RC. ICTV Virus Taxonomy Profile: ascoviridae. J Gen Virol. 2017;98:4–5.
16. Federici BA, Vlak JM, Hamm JJ. Comparative study of virion structure, protein composition and genomic DNA of three ascovirus isolates. J Gen Virol. 1990;71:1661–68.
17. Cheng X, Wan X, Xue J, Moore RC. Ascovirus and Its Evolution. vol. 22. Virol Sin; 2007. p. 137–47.
18. Bigot Y, Asgari S, Bideshi DK, Cheng X, Federici BA, Renault S. Family ascoviridae. In: King AMQ, Adams MJ, Carstens EB, Lefkowitz EJ, editors. Viral Taxonomy, IX Report of the International Committee on the Taxonomy of Viruses. 3rd edn. London: Elsevier–Academic Press; 2011. p. 147–52.
19. Federici BA, Bideshi DK, Tan Y, Spears T, Bigot Y. Ascoviruses: superb Manipulators of Apoptosis for Viral Replication and Transmission. In: Van Etten JL, editor. Lesser Known Large dsDNA Viruses. Berlin, Heidelberg: Springer; 2009. p. 171–96.
20. Zaghloul HAH, Hice RH, Arensburger P, Bideshi DK, Federici BA. Extended in vivo transcriptomes of two ascoviruses with different tissue tropisms reveal alternative mechanisms for enhancing virus reproduction in hemolymph. Sci Rep. 2021;11:16402.
21. Zaghloul HAH, Arensburger P, Federici BA. Host Cytoskeleton Gene Expression Is Correlated with the Formation of Ascovirus Reproductive Viral Vesicles. Viruses. 2022;14:1444.
22. Huang G, Hou D, Wang M, Cheng X, Hu Z. Genome analysis of Heliothis virescens ascovirus 3h isolated from China. Virol Sin. 2017;32:147–54.
23. Noskov V, Kouprina N, Leem S, Koriabine M, Barrett JC, Larionov V. A genetic system for direct selection of gene-positive clones during recombinational cloning in yeast. Nucleic Acids Res. 2002;30:E8.
24. Kouprina N, Noskov VN, Larionov V. Selective isolation of large segments from individual microbial genomes and environmental DNA samples using transformation-associated recombination cloning in yeast. Nat Protoc. 2020;15:734–49.
25. Li S, Wang X, Zhou Z, Zhu J, Hu J, Zhao Y, Zhou G, Huang G. A Comparison of Growth and Development of Three Major Agricultural Insect Pests Infected with Heliothis virescens ascovirus 3h (HvAV-3h). PLoS One. 2013;8.
26. Yu H, Ou-Yang Y, Yang C, Li N, Nakai M, Huang G. 3H-31, A Non-structural Protein of Heliothis virescens ascovirus 3h, Inhibits the Host Larval Cathepsin and Chitinase Activities.. Virol Sin. 2021;36:1036–51.
27. Kouprina N, Larionov V. Selective isolation of genomic loci from complex genomes by transformation-associated recombination cloning in the yeast Saccharomyces cerevisiae. Nat Protoc. 2008;3:371–77.
28. Tidona C, Darai G, eds. The Springer Index of Viruses. New York: Springer; 2011.
29. Blight KJ, Kolykhalov AA, Rice CM. Efficient initiation of HCV RNA replication in cell culture. Science. 2000;290:1972–74.
30. Becker MM, Graham RL, Donaldson EF, Rockx B, Sims AC, Sheahan T, Pickles RJ, Corti D, Johnston RE, Baric RS, et al. Synthetic recombinant bat SARS-like coronavirus is infectious in cultured cells and in mice. Proc Natl Acad Sci U S A. 2008;105:19944–49.
31. Chan LY, Kosuri S, Endy D. Refactoring bacteriophage T7. Mol Syst Biol. 2005;1:2005–18.
32. Larionov V, Kouprina N, Graves J, Chen XN, Korenberg JR, Resnick MA. Specific cloning of human DNA as yeast artificial chromosomes by transformation-associated recombination. Proc Natl Acad Sci U S A. 1996;93:491–96.
33. Gibson DG, Benders GA, Axelrod KC, Zaveri J, Algire MA, Moodie M, Montague MG, Venter JC, Smith HO, Hutchison CAI. One-step assembly in yeast of 25 overlapping DNA fragments to form a complete synthetic Mycoplasma genitalium genome. Proc Natl Acad Sci U S A. 2008;105:20404–09.
34. Knickmann J, Staliunaite L, Puhach O, Ostermann E, Gunther T, Nichols J, Jarvis MA, Voigt S, Grundhoff A, Davison AJ, et al. A simple method for rapid cloning of complete herpesvirus genomes. Cell Rep Methods. 2024;4:100696.
35. Asgari S. Replication of Heliothis virescens ascovirus in insect cell lines. Arch Virol. 2006;15:1689–99.
36. Zaghloul HAH,R, Hice R, Arensburger P, Federici BA. Transcriptome analysis of the *Spodoptera frugiperda* ascovirus in vivo provides insights into how its apoptosis inhibitors and caspase promote increased synthesis of viral vesicles and virion progeny. J Virol. 2017;91:e00874–17.
37. Yu H, Chen H, Li N, Yang C, Xiao H, Chen G, Huang G. Flexible changes to the Heliothis virescens ascovirus 3h (HvAV-3h) virion components affect pathogenicity against different host larvae species. Microbiol Spectr. 2023;11.
38. Peck KM, Lauring AS. Complexities of Viral Mutation Rates. J Virol. 2018;92.
39. Domingo E. Molecular basis of genetic variation of viruses: error-prone replication. Virus as Populations. 2019;35–71.
40. Bailey SF, Morales LAA, Kassen R. Effects of Synonymous Mutations beyond Codon Bias. The Evidence for Adaptive Synonymous Substitutions from Microbial Evolution Experiments. Genome Biol Evol. 2021;13.
41. Oelschlaeger P. Molecular Mechanisms and the Significance of Synonymous Mutations. Biomolecules. 2024;14.

42. Varadaraj K, Skinner DM. Denaturants or cosolvents improve the specificity of PCR amplification of a G + C-rich DNA using genetically engineered DNA polymerases. Gene. 1994;140:1–5.
43. Kumar A, Kaur J. Primer Based Approach for PCR Amplification of High GC Content Gene: mycobacterium Gene as a Model. Mol Biol Internl. 2014;2014:937308.
44. Tran TNT, Labroussaa F, Ebert N, V'Kovski P, Stalder H, Portmann J, Kelly J, Steiner S, Holwerda M, Kratzel A, et al. Rapid reconstruction of SARS-CoV-2 using a synthetic genomics platform. Nature. 2020;582:561.
45. Monttinen HAM, Bicep C, Williams TA, Hirt RP. The genomes of nucleocytoplasmic large DNA viruses: viral evolution writ large. Microb Genom. 2021;7.

Publisher's Note